Whole-Plant Tissue Nitrogen Content Measurement Using Image Analyses in Floriculture Crops[1]

Ranjeeta Adhikari[2] and Krishna Nemali[2,3]

Abstract

Research on image analysis techniques for estimating plant N status in floriculture is limited. We subjected poinsettia (*Euphorbia pulcherrima* Willd. ex Klotzsch) cultivars to five nitrogen concentration treatments for 45 days and captured grayscale images of plants briefly exposed to 450, 625, 660, and 870 nm of light using a multispectral image station. Images were processed to calculate normalized reflectance ratios, including $R_{870/450}$, $R_{870/625}$, and $R_{870/660}$. Dried shoots were analyzed in a laboratory for whole-plant tissue N content ($mg \cdot g^{-1}$). Results indicated that whole-plant N content ranged from 21 to 44 $mg \cdot g^{-1}$ in different N treatments. Among the reflectance ratios, $R_{870/625}$ showed higher correlation with whole-plant N content in different cultivars of poinsettia ($0.72 < r^2 < 0.78$) compared to $R_{870/450}$ and $R_{870/660}$. Based on these results, we custom-built a low-cost image sensor that can be remotely controlled to capture red (625 nm) and near infrared (870 nm) images of plants and transfer images to a cloud storage for processing. The normalized reflectance ratio measured by the image sensor was linearly related to the whole-plant N content (r^2=0.84) and more accurate than soil plant analysis development (SPAD) measurements at predicting plant N status. These results indicate that image analysis in general and images captured by low-cost image sensors can be used for estimation of plant N status in floriculture.

Index words: Chlorophyll, poinsettia, red light reflectance, plant segmentation.

Chemicals used in this study: Water soluble 15-5-15 Cal Mg.

Species used in this study: Poinsettia (*Euphorbia pulcherrima* Willd. ex Klotzsch, cultivars 'Christmas Beauty Marble', 'Christmas Tradition', 'Christmas Glory White', and 'Wintersun White').

Significance to the Horticulture Industry

Plant N status is one of the major determinants affecting growth, development, and quality of floriculture crops. Commonly used methods to measure plant N status are either destructive/ labor-intensive (e.g. laboratory analysis) or expensive (e.g. chlorophyll meters). Although image-based techniques for estimating plant N status are studied extensively in agronomic crops, research on floriculture crops is limited. Our research provides preliminary information on the efficacy of an image analysis technique in general and low-cost image sensors for estimating whole-plant N content in floriculture crops. The information from this research can be used to further develop IoT (internet of things) technologies for measuring whole-plant N status in the future. Such technologies can enable easy measurement of plant N status and timely decisions about fertilizer application in the floriculture industry. This can result in improved crop growth and quality of floriculture crops due to proper N management during production. Further, the technology can result in increased income from reduced wastage of fertilizer and crop losses. In addition, proper fertilizer management can reduce environmental pollution by minimizing fertilizer leaching and runoff from over-fertilizing plants.

Introduction

Floriculture is an important industry in the US with a wholesale value of $4.77 billion (USDA NASS 2019). Nitrogen is an essential element affecting growth, development, and quality of floriculture crops (Leghari et al. 2016). Both sub-optimal and supra-optimal N application rates can negatively affect floriculture crops (Dordas and Sioulas 2008, Kang and van Iersel 2004, Pitchay et al. 2007, Rose and White. 1994). Sub-optimal N rates can result in stunted, yellowish, and poor-quality plants with significant reduction in biomass (Basyouni et al. 2015, Khoddamzadeh and Dunn 2016, Uchida 2005) and delayed flowering (Cox 2016), leading to economic losses (Bullock and Anderson 1998). To avoid N deficiency in plants, growers often over-fertilize plants (Glass 2003). Supra-optimal N application rate leads to excessive growth and increased insect damage (Anusha et al. 2017). Moreover, excess N can be lost from the substrate as nitrates in leachate or runoff (Glass 2003, Raun and Johnson 1999) causing environmental pollution (Biernbaum 1992, Jackson et al. 2009, Uva et al. 1998). In addition, this can result in wastage of N fertilizer, which can increase economic losses (Ali et al. 2017, Mattson 2010).

Floriculture crops are usually grown with a liquid fertilizer containing sufficient amounts of dissolved N. Even when N is supplied at a sufficient concentration in the fertilizer, factors such as plant growth rate, substrate pH, and leaching losses can influence N availability and uptake by plants. Reports indicate that plants absorb and utilize only 30 to 40% of the applied N fertilizer (Glass 2003, Raun and Johnson 1999). Therefore, supplying N based on plant N status is the most effective method. For floriculture crops, optimal tissue N content can vary from 30 to 50 mg per gram of dry matter (Bar-Tal et al. 2001, Nemali and van Iersel 2004, van Iersel et al. 1998, Woodson and Boodley 1983).

Tissue N content can be measured using both direct and indirect methods. The direct method of measuring tissue N

[1]Received for publication August 17, 2020; in revised form December 2, 2021. This research was funded by grant support from the Horticulture Research Institute (HRI), the American Floral Endowment (AFE), and the Fred Gloeckner Foundation.

[2]Department of Horticulture and Landscape Architecture, Purdue University, West Lafayette, IN 47907.

[3]Corresponding author email: knemali@purdue.edu.

content involves analyzing dried plant samples in a laboratory (Dumas 1831, Kjeldahl 1883, Muñoz-Huerta et al. 2013, Pontes et al. 2009). Indirect methods are based on sensors that measure reflectance (e.g. Normalized Difference Vegetation Index sensor, NDVI) and transmittance (e.g. chlorophyll meter) of light received by plants. The indirect methods rely on the relationship between tissue N content and chlorophyll concentration in plants (Muñoz-Huerta et al. 2013). About 25 to 50% of the total N in plants is partitioned to chlorophyll synthesis (Funk et al. 2013; Hikosaka and Terashima 1996). Thus, tissue N content can directly affect chlorophyll synthesis in plants (Evans 1989, Xue et al. 2004). Plant pigments absorb light wavelengths ranging from 380 to 740 nm in photosynthesis (Zhu et al. 2008). Red light (600 to 700 nm) is mostly absorbed by chlorophylls (Sims and Gamon 2003). Therefore, an indirect assessment of plant N status can be made by measuring reflectance and transmittance (both are inversely related to absorption) of red light from a canopy (Erdle et al. 2011, Meyer et al. 1992, Muñoz-Huerta et al. 2013, Thomas and Oerther 1972).

There are challenges associated with both direct and indirect methods of measuring plant N status. Laboratory methods are time-consuming and expensive (Sui et al. 2005). Moreover, laboratory methods involve a destructive harvest and plant loss. Equipment such as a chlorophyll meter can be expensive (Turner and Jund 1994) and may not reflect whole-plant N content (Netto et al. 2002, Xue et al. 2004). Other equipment for indirect assessments (e.g. Normalized Difference Vegetation Index sensor) are not only expensive but are influenced by background color, especially when the plants are small and the canopy is not fully closed (Slater and Jackson 1982, Liu and Huete 1995).

More recently, image analysis-based techniques are becoming popular for estimating plant N status, especially in agronomic crops. Images are comprised of pixels that store information on the intensity of reflected light from an object. Image-processing software can be used to selectively quantify the extent of reflectance of specific wavelengths from plants and estimate plant N status. Image-based platforms equipped with hyperspectral and multispectral cameras are widely used for studying plant N status in agronomic crops and field-grown vegetables (Corti et al. 2017, Leemans et al. 2017, Noh et al. 2006, Tewari et al., 2013). However, research that tested the efficacy of image-based techniques for estimation of plant N status in floriculture crops is limited. The hyperspectral and multispectral imaging techniques are expensive and their adoption in the floriculture industry can be difficult. Image-based methods that are affordable and reliable are unavailable for easy adoption in the floriculture industry. There is an urgent need to conduct preliminary investigations on the efficacy of image-based methods to estimate plant N status and develop affordable and reliable image-based technologies for adoption in the floriculture industry. The objectives of this study were to (1) develop preliminary information on the efficacy of image analysis technique to detect whole-plant N status in floriculture crops using a multi-spectral image station and (2) test a prototype model of an affordable image sensor developed based on the research conducted using the multi-spectral image station.

Materials and Methods

Two experiments were conducted in a temperature and photoperiod-controlled glass greenhouse at Purdue University, West Lafayette, IN during spring of 2018 and 2019 respectively. The first experiment was conducted in spring 2018 to address objective one (above) using a multi-spectral image station (see below for a description). Based on the results from the first experiment, a low-cost image sensor was custom-built (see below for a description) and tested in spring 2019 to address objective two (above).

Plants. In both experiments, four poinsettia cultivars ('Christmas Glory White', 'Christmas Tradition', 'Christmas Beauty Marble', and 'Wintersun White') that differ in plant size and foliage color were tested. 'Christmas Glory White' was comparatively a small plant with a compact growth habit. The plant architecture was an upright V-shape with dark green foliage. 'Christmas Tradition' was a wide V-shaped cultivar with large, pointed, dark-green foliage. 'Wintersun White' was an upright, narrow, V-shaped cultivar with oak-shaped foliage. The leaf color was light green compared to the other cultivars. 'Christmas Beauty Marble' was an upright, medium-sized cultivar with dark green foliage. Poinsettia was used as the test plant in our study due to its popularity and high N requirement during growth. Unrooted cuttings of the poinsettia cultivars were obtained from a commercial company (Ball Horticultural Co., IL, U.S.). Cuttings were dipped in 0.1% indole butyric acid rooting hormone (Rhizopon® AA #, Earth City, MO, U.S.) before inserting into 48-cell pack inserts (Greenhouse Megastore, Danville, IL, U.S.) filled with the propagation mix (Fafard® Germinating Mix, Sungro Horticulture, Agawam, MA, U.S.). The cell packs with cuttings were placed under a mist for three weeks to ensure rooting. Rooted cuttings were transplanted into containers 15.2 cm (6 in) tall and 1.33 L (45 fl oz) in volume (Greenhouse Megastore, Danville, IL, U.S.) filled with a soilless substrate containing 75% peat, 20% perlite and 5% vermiculite (Sunshine Mix # 8, Sungro Horticulture, Agawam, MA, U.S.). During the two experiments, the greenhouse was maintained at an average temperature of 25.4 ± 0.4/ 20.4 ± 0.3 C (78/69 F) (day/night) and a daily light integral of 11.3 ± 0.7 $mol \cdot m^{-2} \cdot d^{-1}$. A photoperiod of 18 h was maintained using high-pressure sodium supplemental lights to ensure that the plants remained in the vegetative stage.

Production system. Plants were grown in a custom-built ebb and flow sub-irrigation system in both experiments. The system was built by connecting low-rise flood tables (1.22 m × 1.22 m or 4 ft × 4 ft; Active Aqua, Hydro farm, CA, U.S.) to reservoirs (151.4 L or 40 gal; Active Aqua) using flexible poly-vinyl tubing (1.9 cm or 0.75 in ID, Everbilt Co., Home Depot, Atlanta, GA, U.S.) and submersible pumps (18.9 LPM or 300 GPH; Total Pond, West Palm Beach, FL, U.S.). Each reservoir contained one

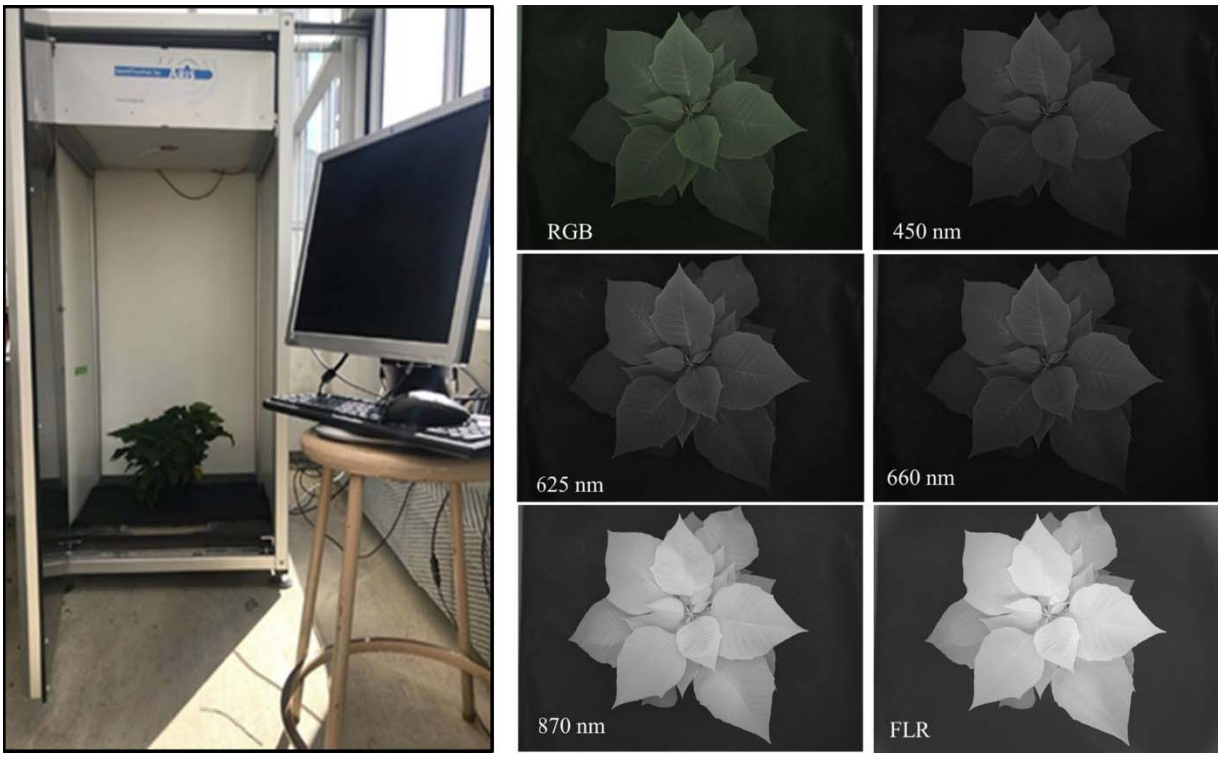

Fig. 1. Multispectral image station used to capture images of plants (left). Captured images (right) were saved in the computer attached to the image station. Gray scale images of 450, 625, 660, and 870 nm are shown in addition to the color (RGB) image. The FLR image was captured using chlorophyll fluorescence emitted by the plant, after exposing plants to 450 nm and collecting reflectance of wavelengths greater than 695 nm.

submersible pump and there was one reservoir for each ebb and flow tray. An irrigation timer (Titan Controls Apollo 6, Hawthorne Gardening Company, Vancouver, WA, U.S.) was used to turn-on the pumps every day for a period of 15 min. Nutrient solution was supplied to plants on the first day while tap water was supplied during the remaining days of the week. This was done to ensure that plants in different fertilizer treatments (see *Treatments* section below) showed distinct tissue N levels at harvest. The water inlet to the flood table was wider (1.9 cm or 0.75 in) than the outlet (1.3 cm or 0.5 in), which resulted in maintaining approximately 3 cm (1.18 in) deep solution in the tray when submersible pumps were turned-on during irrigation. Substrate absorbed the solution through the bottom holes of the container by capillary action. The duration of each irrigation event (15 min) was sufficient to increase moisture content of the substrate close to container capacity. Solution drained back to the reservoir through both the inlet and outlet of the tray due to gravity after the pumps were turned off. Each low-rise flood tables contained eight plants consisting of two plants from each cultivar.

Treatments. In the first experiment, plants were subjected to five fertilizer rates by supplying nutrient solutions with different electrical conductivity (EC) levels of 0.75, 1.5, 2.5, 3.5 and 4.5 $dS{\cdot}m^{-1}$ once a week (containing N levels of 109, 217, 362, 507 and 652 mg $N{\cdot}L^{-1}$, respectively). A water-soluble fertilizer containing 15N:2.2P:12.5K (15-5-15 Cal Mg, Peter's Excel, ICL Specialty Fertilizer, UK) was used to prepare different fertilizer rates. Fresh fertilizer solution was prepared every week and recirculated through the sub-irrigation system on the first day of the week. Substrate EC levels were 1.0 ± 0.12, 1.7 ± 0.11, 2.1 ± 0.15, 2.9 ± 0.15, and 3.7 ± 0.15 in the 0.75, 1.5, 2.5, 3.5 and 4.5 $dS{\cdot}m^{-1}$ treatments, respectively. The pH of the substrate ranged from 5.5 to 6.5 during the trial. In the second experiment, plants were exposed to three fertilizer treatments by supplying nutrient solutions with different EC levels of 0.75, 2.5, and 4.5 $dS{\cdot}m^{-1}$ once a week. The fertilizer and application method were same as in the first experiment. The substrate EC was not measured in the second experiment; however, substrate pH was maintained in the range of 5.4 to 6.4 during the treatment phase.

Image capture and processing. In the first experiment, images of plants were collected a day before harvest using a multispectral image station (TopView, Aris, Eindhoven, The Netherlands; Fig. 1). The dimensions of the image station were 1.83 m × 0.61 m × 0.46 m. Individual plants from the two experiments were placed inside the image station and sequentially exposed to low intense wavebands of 450, 625, 660, and 870 (± 20) nm inside the image station using strobed-light-emitting diodes (LEDs; OSLON SSL80, Osram, Munich, Germany; 24 per waveband). The lights were automatically turned on and off by a microcontroller (Arduino UNO, Adafruit, NY, U.S.). The exposure period was approximately 30 milliseconds for a given waveband, during which time a monochromatic camera (acA3800; Basler Ace, 10 MP with MT9J003 CMOS sensor, ON Semiconductor, AZ, U.S.) connected to

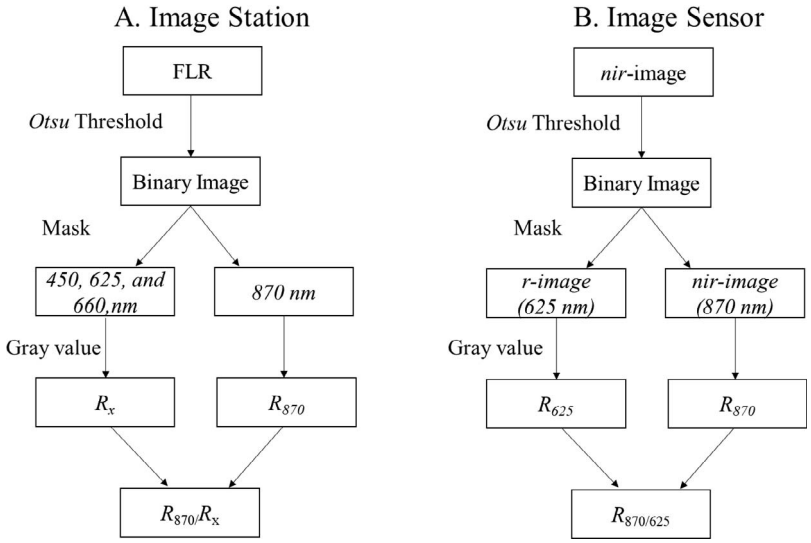

Fig. 2. Image processing logic used for measuring normalized reflectance ratio using image station (A) and image sensor (B). The FLR or *nir*-image were used to develop binary images, which were used to mask the background and filter for plant pixels in images. Average gray or reflectance value was estimated for the segmented gray scale images and normalized reflectance ratios were calculated.

the microcontroller and located at the top of the station captured images (Fig. 1). In addition, plants were exposed a second time for a period of 800 milliseconds to blue light (450 nm) for exciting chlorophyll to fluoresce. The fluorescence image (FLR) was captured using a long-band pass filter (>695 nm). The images captured for each wavelength exposure have identical resolution (pixel number). The images were stored in a computer connected to the image station.

In the first experiment, images were processed automatically using built-in software (MultiSpec software V2.0, Aris, The Netherlands). Processing involved separating plant pixels from the background in each image and measuring average reflectance from the plant when exposed to different wavelengths (Fig. 2A). The FLR image was used to develop a binary image containing black (background) and white (plant) regions. For background separation, the binary image was used to filter for plant pixels in the gray scale images. Grayscale images were 8-bit depth with 2^8 (or 256) levels of gray values. The average gray value (R), a measure of average plant reflectance, of an image was expressed on a relative scale of 0 to 255 using the following equation:

$$R = \frac{[(GV_1 \times PN_1) + \cdots + (GV_n PN_n)]}{N} \quad [1]$$

In Eq. [1], $GV_1, \ldots, GV_n$ are specific classes (0 - 255) of gray values, $PN_1, \ldots, PN_n$ are number of pixels associated with each gray class, and N is total number of pixels ($PN_1 + \ldots + PN_n$).

Intensity of light reflected from a plant and average gray value of an image can be affected by plant height (e.g. taller vs shorter plant). More reflected light is captured when a plant is taller and closer to the camera than a shorter plant. Therefore, height differences between individual plants can confound plant reflectance measurements from an image. As near infrared light is mostly reflected and not used by plants (Basyouni and Dunn 2013, Gausman 1974), plant reflectance in the visible bands (i.e., 450, 625, and 660 nm) was normalized to the reflectance in the near infrared band (870 nm) to account for differences in plant height. Normalized reflectance ratios for individual visible wavelengths (x) were calculated using the following equation:

$$R_{870/x} = \frac{R_{870}}{R_x} \quad [2]$$

In Eq. [2], R_{870} is reflectance measured from plants exposed to 870 nm (near infrared light) and R_x is reflectance measured from plants exposed to visible wavelengths (x, nm).

In the second experiment, a low-cost image sensor (Fig. 3) was custom-built to capture images based on information generated from the first experiment. The image sensor was built using micro-controllers (Raspberry Pi 3, Raspberry Pi Foundation, Bells Yew Green, East Sussex, UK), miniature cameras (Raspberry Pi NoIR Module V2, Sony IMX219 8-megapixel sensor) and band-pass light filters (12.5 mm diameter; Edmund Optics Inc., NJ, U.S.) for red (*r*, 625 ± 10 nm) and near-infrared (*nir*, 870 ± 10 nm) light. The components were enclosed inside a plastic Raspberry Pi casing (9 cm × 6 cm or 3.54 in × 2.36 in Smarticase, Part# 31AC3455, Newark, An AVNET Company, IL, U.S.). Cameras were placed in two separate black Pi camera cases (3.5 cm × 3 cm or 1.38 in × 1.18 in, Newark, An AVNET Company, Chicago, IL, U.S.), which were mounted side-by-side on the Raspberry Pi casing. The camera cases contained a square hole in the middle for the lens view. A flex cable was used to connect the cameras to the microcontroller through slits on the casings. As filters were cylindrical in shape, a black foam (2 cm × 2 cm or 0.79 in × 0.79 in) with a circular hole in the middle and the sticky side was adhered to the top of the camera case. Filters were snugly inserted into the circular hole such that only filtered light reached the camera sensor.

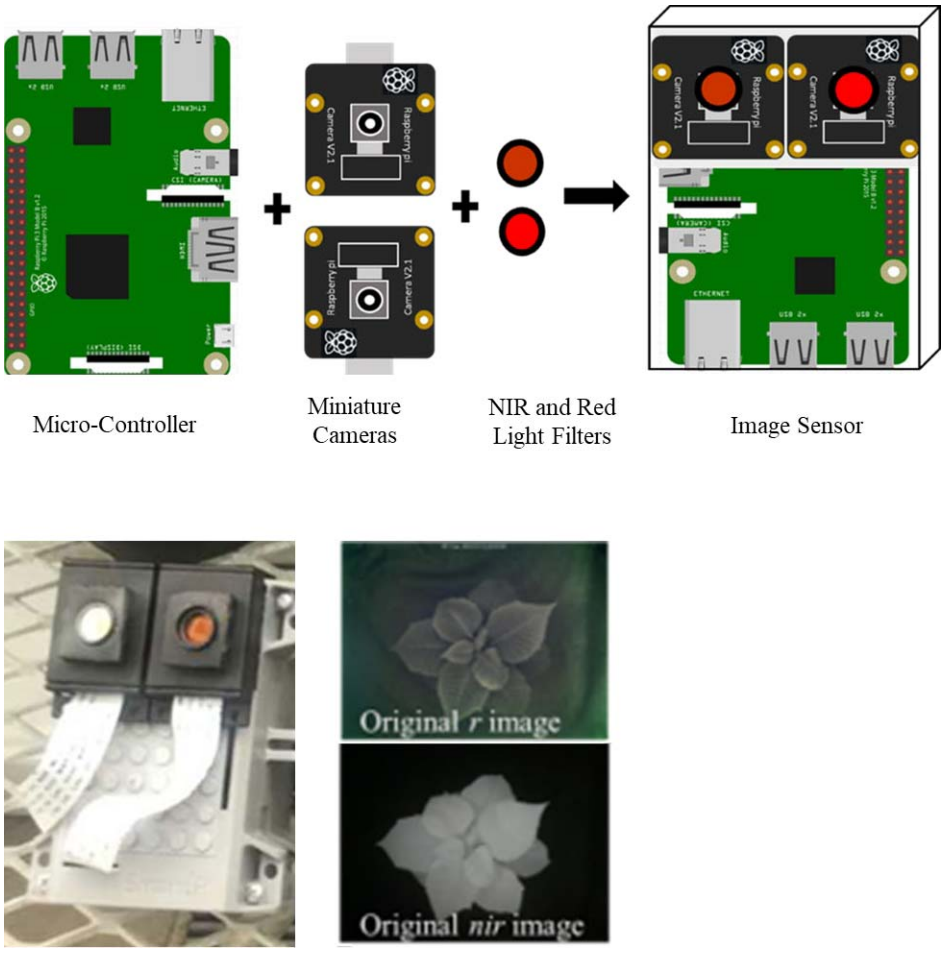

Fig. 3. Components used to custom build a low-cost image sensor (top row) and picture of the actual image sensor and red (*r*, 625 nm) and near infrared (*nir*, 870 nm) images captured by the sensor (bottom row).

In the second experiment, plants were imaged a day before harvest. Plant images were collected inside the greenhouse during early morning (8:00 am) or late afternoon (5:00 pm) when fluctuations in sunlight intensity are usually less. The image sensor was placed approximately 30 cm (12 in) above the plants for capturing images. The filters on the cameras allowed *r* and *nir* wavelengths of light reflected from plants to reach the camera sensor, thereby enabling capture of *r*- and *nir*-images of plants. The image sensor can be remotely connected to a computer using a web interface (Rpi-Cam-Web-Interface, Raspberry Pi Foundation). The interface allows the computer to remotely control the cameras connected to the microcontrollers, view images on the desktop, and capture and transfer images to a cloud storage. The captured images were saved using specific file names on a cloud storage (DropBox Inc., CA, U.S.). The resolution of stored *r*- and *nir*-images were 4- (2309 × 1732) and 5- (2592 × 1944) mega pixels respectively, each with an 8-bit depth.

In the second experiment, images were processed using custom-coded software (MATLAB 2018b, Mathworks Inc., MA, U.S.) on the computer. Image processing (Fig. 2B) involved separating the background from the plants, measuring average plant reflectance in the *r*- and *nir*-images, and calculating a normalized reflectance value as in the first experiment. As plants reflect more near infrared light than the background, plant pixels appear bright and background pixels appear dark in the *nir*-image. The contrast between the plant and background in the *nir*-image was used for background separation. A binary image was generated from the *nir*-image using the 'Otsu' thresholding technique (Otsu 1979). The binary image was used as a 'mask' to separate plant pixels from the background. Gray values of plant pixels were extracted and average grey value of *r* (R_{625}) and *nir* (R_{870}) images was calculated. From these, a reflectance ratio ($R_{870/625,\ sensor}$) was calculated as:

$$R_{870/625\ (sensor)} = \frac{R_{870}}{R_{625}}$$

Other measurements. In both experiments, photosynthetic photon flux density during different days was measured using quantum sensors (Li-190 R, Li-COR, Lincoln, NE, USA). Day and nighttime temperatures were measured using thermistors (ST-100, Apogee Instruments, Inc., Logan, UT, U.S.). Environmental data was measured hourly by connecting the quantum sensor and thermistors to a datalogger (CR 1000, Campbell Scientific, Logan, UT, U.S.). The EC of the fertilizer solution and substrate were measured using a dielectric sensor (5TE, Meter Group, WA, U.S.) connected to a handheld monitor. In both experiments, SPAD readings were measured on 5-6 leaves

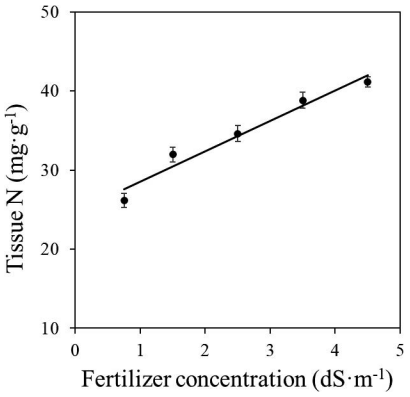

Fig. 4. Linear relationship between laboratory analyzed whole-plant N content (Tissue N) and fertilizer concentration supplied to poinsettia, averaged across cultivars. A linear regression was fitted to the variables using data from all four cultivars. LSMeans and standard error (n = 12) are shown. The fitted equation is $R_{ratio} = 24.7 + 3.84$. Fert. Conc., $r^2 = 0.72$.

from each plant and averaged using SPAD-502 (Konica Minolta Inc., Osaka, Japan) during the same time when plant images were collected.

In both experiments, plants were harvested after 45 days from transplanting. Plant shoots were dried in a forced air oven for one week at 70 C (158 F). Entire dried shoots from a plant were ground into a fine powder and samples from different replications were sent to a commercial laboratory (A & L Great Lakes, Fort Wayne, IN, U.S.) for measuring whole-plant N content.

In the first experiment, the dried shoot samples were weighed to measure shoot dry weight (SDW). The optimal fertilizer solution concentration resulting in a maximum SDW was calculated as the second derivative of the fitted function between SDW and fertilizer concentration.

Experimental design and statistical analyses. Both experiments used a split-plot design with fertilizer treatment as the main-plot and cultivar as the sub-plot with three replications in the first and four replications in the second experiment. Fertilizer treatments were randomized within each replication and cultivars were randomized within each fertilizer treatment. An experimental unit comprised of a plant belonging to a cultivar within a fertilizer treatment in a replication. Data were analyzed for main and interaction effects using the general linear model of statistical analysis software (SAS, Version 9.4, SAS Institute, Cary, NC) with appropriate error terms for the main and split-plots. Relationship between any two variables was tested using the linear regression procedure of SAS.

Results and Discussion

Whole-plant N content (first experiment). A linear increase in whole-plant N content with increasing fertilizer concentration was observed in all cultivars (Fig. 4). A linear relationship between tissue N content and fertilizer concentration was previously reported in poinsettia (Wright et al. 1990, Rose and White 1994). The slope of the relationship between whole-plant N content and fertilizer concentration indicates that plant N level in poinsettia cultivars increased by 3.84 $mg \cdot g^{-1}$ (or 0.384%) for an increase in EC of 1.0 $dS \cdot m^{-1}$ (or 144.9 mg $N \cdot L^{-1}$ supplied weekly to plants, based on the relationship between N concentration in the fertilizer and EC). Whole-plant N levels measured in different fertilizer rates ranged between 21 to 44 $mg \cdot g^{-1}$ (2.1 to 4.4%). This indicates that a wide range of tissue N levels were observed in plants from different fertilizer rates. The wide range is a pre-requisite for developing algorithms between plant N status and image-derived reflectance ratio. There were no significant differences in whole-plant N content among cultivars in a given fertilizer rate. This suggests that N uptake efficiency (ratio of N in plant tissue to that supplied in the fertilizer) was likely not different among cultivars.

Plant growth (first experiment). Shoot dry weight of poinsettia cultivars showed a curvilinear response to increasing fertilizer concentration (Fig. 5). A decline in SDW was observed in the low (0.75 and 1.5 $dS \cdot m^{-1}$) and high (4.5 $dS \cdot m^{-1}$) fertilizer concentration treatments, indicating both sub- or supra-optimal levels of fertilizer concentration can negatively affect plant growth. A curvilinear response of SDW to increasing fertilizer concentration was previously reported in floriculture crops (Kang and van Iersel 2004, Pitchay et al. 2007, Rose and White 1994). While N limitation mostly caused a reduction in plant growth in the two low fertilizer concentrations, increased osmotic stress from excessive concentration of dissolved fertilizer salts in the root zone is likely the reason for a decrease in plant growth in the highest fertilizer concentration. Further, the results support the concept that supplying excessive fertilizer concentrations to avoid N deficiencies can negatively affect crop growth. The interaction between cultivar and fertilizer treatment on SDW of poinsettia was significant (Fig. 5). This indicates that the response of SDW to fertilizer concentration varied among cultivars. A more pronounced decrease in SDW was observed in two of the four cultivars ('Christmas Tradition' and 'Wintersun White') in the two lowest fertilizer concentrations. This suggests increased sensitivity to lower fertilizer concentrations in these two cultivars compared to the other cultivars. Interestingly, these cultivars also were larger based on SDW (Fig. 5). It is likely that the demand for N is relatively higher in these cultivars due to their larger size, which may have resulted in a relatively larger decline in growth when supplied with lower concentrations of N in the fertilizer. The optimal fertilizer concentration for maximum SDW ranged between 2.8 to 3.2 $dS \cdot m^{-1}$ (based on the second derivative of fitted functions) among the four cultivars. When translated to plant N status (based on the fitted linear relationship in Fig. 4), the equivalent optimal range of whole-plant tissue N concentration was 35.5 to 37 $mg \cdot g^{-1}$ for the poinsettia cultivars. Our results on optimal tissue N content for poinsettia are close to the previously reported range of 38 to 41 $mg \cdot g^{-1}$ (Rose and White 1994, Wright et al. 1990). Based on the range of tissue N levels observed (21 to 44 $mg \cdot g^{-1}$), plants in our study experienced sub-optimal, optimal, and supra-optimal tissue N levels.

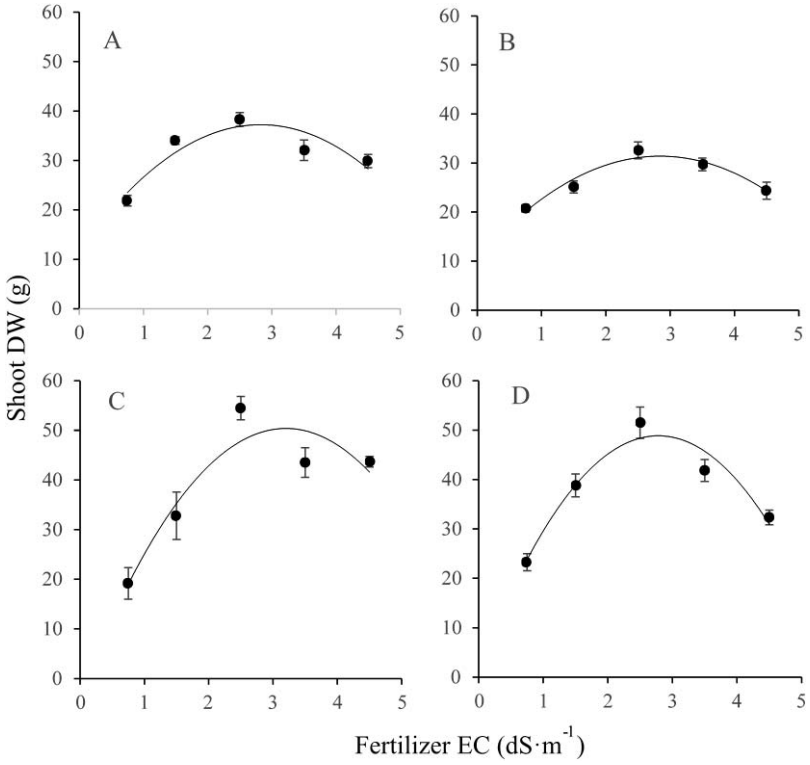

Fig. 5. Relationship between shoot dry weight (Shoot DW) and fertilizer concentration (Fertilizer EC) in different poinsettia cultivars: A. 'Christmas Beauty Marble' (CBM), B. 'Christmas Glory White' (CGW), C. 'Christmas Tradition' (CT), and D. 'Wintersun White' (WW). Fitted equations were $SDW_{CBM} = 11.8 + 18.01 \cdot EC - 3.189 \cdot EC^2$ ($r^2 = 0.72$), $SDW_{CGW} = 10.5 + 14.68 \cdot EC - 2.582 \cdot EC^2$ ($r^2 = 0.77$), $SDW_{CT} = 3.1 + 33.41 \cdot EC - 5.218 \cdot EC^2$ ($r^2 = 0.76$), and $SDW_{WW} = 1.9 + 33.78 \cdot EC - 6.073 \cdot EC^2$ ($r^2 = 0.84$).

Whole-plant plant N content vs. normalized reflectance ratios (first experiment). Normalized reflectance values ranged between 4.0 to 5.5, 3.0 to 4.5, and 3.5 to 5.0 for $R_{870/450}$, $R_{870/625}$, and $R_{870/660}$, respectively (Fig. 6). The higher range of normalized reflectance values observed for $R_{870/450}$ is likely due to relatively higher absorption or lower reflectance of blue than red wavelengths by plants (McCree 1971). Blue light is absorbed by other pigments (e.g. carotenoids) in addition to chlorophylls, which increases overall blue light absorption by plants. Positive and linear relationships were observed between the laboratory measured whole-plant N content and normalized reflectance ratios ($0.38 < r^2 < 0.56$) when data from all four cultivars were pooled (Fig. 6 A-C). A correlation between tissue N content and spectral reflectance was shown in other crops (Li et al. 2008, Peñuelas and Filella 1998). Significant *P*-values in our study indicate a true relationship between whole-plant N content and normalized reflectance ratios. The interaction between cultivar and fertilizer rates for whole-plant tissue N content and the normalized reflectance ratio was not significant.

Results further indicated that among the three normalized reflectance ratios, $R_{870/625}$ showed the highest prediction accuracy ($r^2 = 0.56$, Fig. 6B) when data from all four cultivars were pooled. Chlorophyll concentration is affected by plant N status (Muñoz-Huerta et al. 2013) and the chlorophyll level can affect plant reflectance (Thomas and Gausman 1977).The normalized reflectance ratio of $R_{870/625}$ was more closely related to tissue N content in part because red light absorption or reflectance is mostly affected by chlorophylls (and not by other pigments such as carotenoids and anthocyanins). Similar results have been reported earlier (Albayrak 2008). Although chlorophyll absorption peaks in the blue waveband, $R_{870/450}$ was poorly correlated with whole-plant N content. This may be due to the influence of carotenoids on blue absorbance/reflectance, and carotenoids are less affected by tissue N content compared to chlorophyll (Gitelson et al. 2002). Chlorophyll absorption of light sharply decreases at wavebands that are greater than 680 nm (McCree 1971). It is possible that some of the wavebands included in 660 nm treatment fell outside the limit of 680 nm due to spectral properties of LEDs used inside the image station. This may have affected chlorophyll absorption and subsequently prediction accuracy of $R_{870/660}$.

Prediction accuracy of R_{870}/R_{625} was further increased ($0.72 < r^2 < 0.78$) when the relationship between whole-plant N content and $R_{870/625}$ was analyzed separately for each cultivar (Fig. 7 A-D). Cultivars in our study were chosen based on inherent differences in plant architecture and foliage color. A larger spread, and thus relatively lower prediction accuracy, is likely to happen when data from all cultivars with inherent differences are used in the regression analyses. Therefore, cultivar-specific algorithms can predict whole-plant N content more accurately than species-specific algorithms using image analyses.

Regression analyses indicated a significant inverse relationship between whole-plant N content and R_{625} (r^2

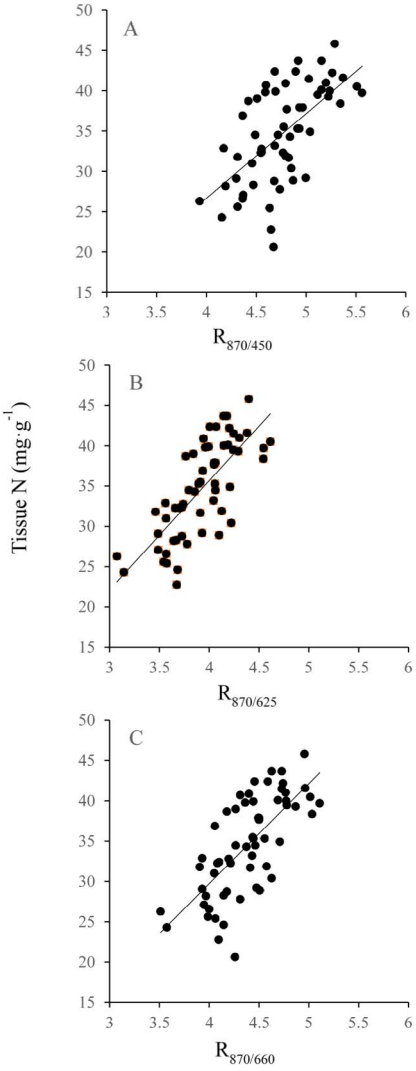

Fig. 6. Relationship between whole-plant N content (Tissue N) and normalized reflectance ratios obtained from images exposed to 450, 625, and 660 nm. A. Tissue N vs. $R_{870/450}$, B. Tissue N vs. $R_{870/625}$, and C. Tissue N vs. $R_{870/660}$. Fitted equations are Tissue N = -15.3 + 10.48· $R_{870/450}$ (r^2 = 0.38), Tissue N = -19.7 +13.3· $R_{870/625}$ (r^2 = 0.56), Tissue N = -19.9 +12.43·$R_{870}/_{660}$ (r^2 = 0.49), averaged across poinsettia cultivars.

$= 0.51$, $P < 0.001$, Fig. 8A) and no significant relationship between whole-plant N content and R_{870} ($r^2 = 0.004$, Fig. 8B) in the poinsettia cultivars. This indicates that whole-plant N content estimation using $R_{870/625}$ is biologically related to red light absorption by plants. Nearly 25 to 50% of total N absorbed by plants is partitioned to chlorophyll (Funk et al. 2013, Hikosaka and Terashima 1996), thus whole-plant N content can directly affect chlorophyll synthesis in plants (Evans 1989, Moorby and Besford 1983, Xue et al. 2004). Because red wavelengths (620-680 nm) are mostly absorbed by chlorophyll (Gates et al. 1965, Sims and Gamon 2003), changes in chlorophyll concentration (due varying tissue N levels) can decrease or increase absorption of red light received by plants (Munden et al. 1994). No relationship between whole-plant N content and R_{870} is expected as near infrared light is mostly reflected and not absorbed by plants (Basyouni and Dunn 2013). Based on the optimal whole-plant N content

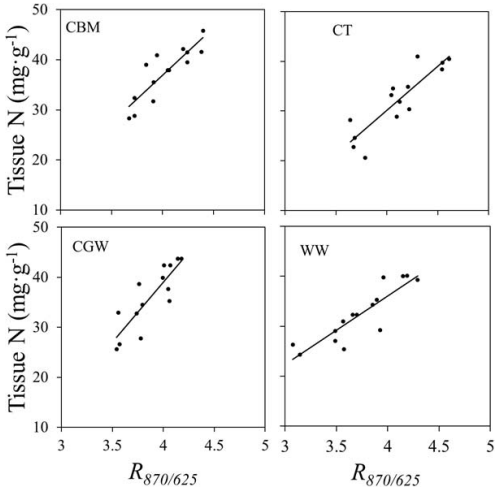

Fig. 7. Relationship between laboratory analyzed whole-plant nitrogen content (Tissue N) and reflectance ratio ($R_{870/625}$) in different poinsettia cultivars: 'Christmas Beauty Marble' (CBM), 'Christmas Glory White' (CGW), 'Christmas Tradition' (CT), and 'Wintersun White' (WW). Fitted equations are Tissue N_{CBM} = -38.5 + 18.8·$R_{870/625}$ (r^2 = 0.75), Tissue N_{CT} = -40.8 + 17.74·$R_{870/625}$ (r^2 = 0.78), Tissue N_{CGW} = -56.6 + 23.90·$R_{870/625}$ (r^2 = 0.72), and Tissue-N_{WW} = 18.9 + 13.76·$R_{870/625}$, (r^2 = 0.77).

of 35.5 to 37 mg·g^{-1} identified in our study, the recommended range of $R_{870/625}$ for poinsettia cultivars is calculated as 4.1 to 4.3 (using the fitted function in Fig. 6B). The $R_{870/625}$ value can aid in maintaining optimal plant N status in poinsettia cultivars using an image analysis technique.

Low-cost image sensor (second experiment). Based on the above results, the normalized reflectance ratio of R_{870}/R_{625} measured by a multispectral image station can be used for estimation of whole-plant tissue N content with reasonable accuracy. However, a multispectral image station can be expensive and may not be affordable to growers. Moreover, plants should be moved into the image station for estimating tissue N content, which can be labor intensive in medium and largescale operations. Therefore, we built an affordable image sensor (approximately $200), developed the relationship between tissue N content and the image sensor derived reflectance ratio, and tested the

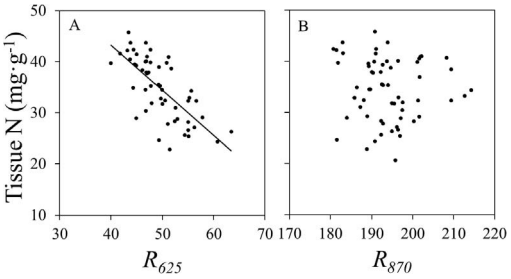

Fig. 8. Relationship between A. whole-plant nitrogen content (Tissue N) and average plant reflectance of red waveband (625 nm, R_{625}) and B. tissue N and average plant reflectance of near infrared waveband (870 nm, R_{870}), averaged across poinsettia cultivars. Fitted linear regression was Tissue N = 78.5 – 0.88· R_{620} (r^2 = 0.51).

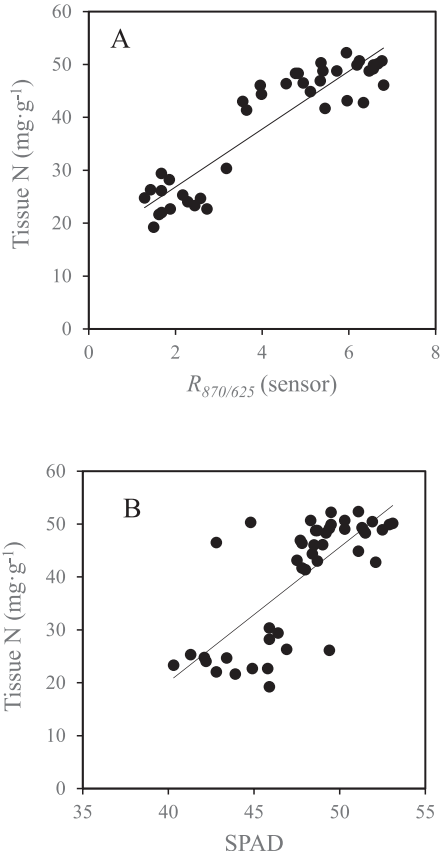

Fig. 9. Relationship between A. whole-plant nitrogen content (Tissue N) and reflectance ratio ($R_{870/625,\ sensor}$) measured by the image sensor [Tissue N = 15.9 + 5.47·$R_{870/625}$ (r^2 = 0.84)], and B. tissue N and soil plant analysis development (SPAD) measurements [Tissue N = 81.8 + 2.55·SPAD (r^2 = 0.56)] and averaged across poinsettia cultivars.

efficacy of the custom-built image sensor to estimate whole-plant N content of poinsettia cultivars by comparing it with SPAD measurements in the second experiment.

Across all cultivars, there was a linear and positive relationship between laboratory-measured whole-plant tissue N content and $R_{870/625}$ obtained using the custom-built low-cost image sensor (Fig. 9A). This indicates that a low-cost image sensor can be used to reliably estimate tissue N content. Statistical analyses also indicated that the relationship between whole-plant tissue N content and SPAD measurements was linear and positive across all four cultivars (Fig. 9B). However, the relationship was stronger for $R_{870/625\ (sensor)}$ than that of SPAD. The relation between whole-plant N content and SPAD had an r^2 of 0.56 whereas that between whole-plant N content and $R_{870/625,\ sensor}$ was 0.84. This indicates that the image sensor measurement can predict tissue N content more accurately than SPAD measurements. Moreover, the cost of the image sensor is many folds lower than that of a SPAD meter and image sensor measurements provide a more accurate estimate of whole-plant N status compared to leaf level estimates using a SPAD meter. Further information related to elemental specificity of low-cost image sensor and the relationship between chlorophyll concentration and $R_{870/625\ (sensor)}$ can be found elsewhere (Adhikari et al. 2020).

In conclusion, the intention of our study was to generate preliminary information using a multispectral image station on the efficacy of an image analysis technique and suitable wavelengths for estimating plant N status in floriculture crops. Further, we intended to test the efficacy of a low-cost image sensor, which was custom-built based on the preliminary information from the multispectral image station. We demonstrated that image-based reflectance measurements can be used to indirectly estimate whole-plant N content in floriculture crops. Our study conducted using the multispectral image station revealed that reflectance index R_{870}/R_{625} was most suitable for estimating whole-plant N content compared to other ratios such as R_{870}/R_{450} and R_{870}/R_{660}. In addition, the normalized reflectance ratio measured by the low-cost image sensor was highly correlated with laboratory-based whole-plant tissue N content values and was found to be more accurate than SPAD measurements at predicting plant N status. We hope that our study provides bases for more experimentation in the future on the applicability of image analysis techniques in floriculture production.

Literature Cited

Adhikari, R., C. Li, K. Kalbaugh, and K. Nemali. 2020. A low-cost smartphone controlled sensor based on image analysis for estimating whole-plant tissue nitrogen (N) content in floriculture crops. Computers and Electronics in Agriculture. DOI: https://doi.org/10.1016/j.compag.2019.105173.

Albayrak, S. 2008. Use of reflectance measurements for the detection of N, P, K, ADF and NDF contents in sainfoin pasture. Sensors 8(11):7275–7286.

Ali, M.M., A. Al-Ani, D. Eamus, and D.K. Tan. 2017. Leaf nitrogen determination using non-destructive techniques–A review. J. Plant Nutr. 40(7):928–953.

Anusha, S., G.P. Rao, and D.S.R. Kumar. 2017. Effect of different nitrogen doses on sucking pests and yield in Bt cotton under unprotected and protected conditions. J. Entomol. and Zoology Studies. 5(2):611–6152017.

Bar-Tal, A., B. Aloni, L. Karni, and R. Rosenberg. 2001. Nitrogen nutrition of greenhouse pepper. II. Effects of nitrogen concentration and NO3: NH4 ratio on growth, transpiration, and nutrient uptake. HortScience 36(7):1252–1259.

Basyouni, R. and B. Dunn. 2013. Use of reflectance sensors to monitor plant nitrogen status in horticultural plants. Oklahoma Cooperative Extension Service HLA-6789:1-4.

Basyouni, R., B.L. Dunn, and C. Goad. 2015. Use of nondestructive sensors to assess nitrogen status in potted poinsettia (*Euphorbia pulcherrima* L. (Willd. ex Klotzsch)) production. Scientia Horticulturae 192:47–53.

Biernbaum, J.A. 1992. Root-zone management of greenhouse container-grown crops to control water and fertilizer. HortTechnology 2(1):127–132.

Bullock, D.G., and D.S. Anderson. 1998. Evaluation of the Minolta SPAD-502 chlorophyll meter for nitrogen management in corn. J. Plant Nutr. 21(4):741–755.

Corti, M., P.M. Gallina, D. Cavalli, and G. Cabassi. 2017. Hyperspectral imaging of spinach canopy under combined water and nitrogen stress to estimate biomass, water, and nitrogen content. Biosystems Eng. 158:38–50.

Cox, D. 2016. Soil fertility for field grown cut flowers. University of Massachusetts Amherst. https://ag.umass.edu/greenhouse-floriculture/fact-sheets/soil-fertility-for-field-grown-cut-flowers. Accessed February 25, 2021.

Dordas, C.A., and C. Sioulas. 2008. Safflower yield, chlorophyll content, photosynthesis, and water use efficiency response to nitrogen fertilization under rainfed conditions. Industrial crops and Products 27(1):75–85.

Dumas, J.B.A. 1831. Procedes de l'analyse organic. Ann. Chim. Phys. 247:198–213.

Erdle, K., B. Mistele, and U. Schmidhalter. 2011. Comparison of active and passive spectral sensors in discriminating biomass parameters and nitrogen status in wheat cultivars. Field Crops Res. 124(1):74–84.

Evans, J.R. 1989. Photosynthesis and nitrogen relationships in leaves of C 3 plants. Oecologia 78(1):9–19.

Funk, J.L., L.A. Glenwinkel, and L. Sack. 2013. Differential allocation to photosynthetic and non-photosynthetic nitrogen fractions among native and invasive species. PloS one 8(5):e64502.

Gates, D.M., H.J. Keegan, J.C. Schleter, and V.R. Weidner. 1965. Spectral properties of plants. Appl. Optics 4(1):11–20.

Gausman, H.W. 1974. Leaf reflectance of near infrared. Photogrammetric Eng. 40(2):183–191.

Gitelson, A.A., Y. Zur, O.B. Chivkunova, and M.N. Merzlyak. 2002. Assessing Carotenoid Content in Plant Leaves with Reflectance Spectroscopy. Photochemistry and Photobiology 75(3):272–281.

Glass A.D. 2003. Nitrogen use efficiency of crop plants: physiological constraints upon nitrogen absorption. Critical Reviews in Plant Sci. 22(5):453–470.

Hikosaka, K. and I. Terashima. 1996. Nitrogen partitioning among photosynthetic components and its consequence in sun and shade plants. Functional Ecol. 10:335–343.

Jackson, B.E., R.D. Wright, and M.M. Alley. 2009. Comparison of fertilizer nitrogen availability, nitrogen immobilization, substrate carbon dioxide efflux, and nutrient leaching in peat-lite, pine bark, and pine tree substrates. HortScience 44(3):781–790.

Kang, J.G. and M.W. van Iersel. 2004. Nutrient solution concentration affects shoot: root ratio, leaf area ratio, and growth of sub irrigated salvia (*Salvia splendens*). HortScience 39(1):49–54.

Khoddamzadeh, A.A. and B.L. Dunn. 2016. Application of optical sensors for nitrogen management in Chrysanthemum. HortScience 51(7):915–920.

Kjeldahl, J.G.C.T. 1883. New method for the determination of nitrogen in organic bodies. J. Anal. Chemistry 22(1):366–382.

Leemans, V., G. Marlier, M.F. Destain, B. Dumont, and B. Mercatoris. 2017. Estimation of leaf nitrogen concentration on winter wheat by multispectral imaging. *In*: Hyperspectral Imaging Sensors: Innovative Applications and Sensor Standards 2017 April 28 (Vol. 10213, p. 102130I). Intl. Soc. for Optics and Photonics.

Leghari, S.J., N.A. Wahocho, G.M. Laghari, A. HafeezLaghari, G. MustafaBhabhan, K. HussainTalpur, T.A. Bhutto, S.A. Wahocho, and A.A. Lashari. 2016. Role of nitrogen for plant growth and development: A review. Adv. in Environ. Biol. 10(9):209–219.

Li, F., M.L. Gnyp, L. Jia, Y. Miao, Z. Yu, W. Koppe, G. Bareth, X. Chen, and F. Zhang. 2008. Estimating N status of winter wheat using a handheld spectrometer in the North China Plain. Field Crops Res. 106(1):77–85.

Liu, H.Q. and A. Huete. 1995. A feedback-based modification of the NDVI to minimize canopy background and atmospheric noise. IEEE Transactions on Geoscience and Remote Sensing 33(2):457–465.

Mattson, N. 2010. What's your fertilizer costs? http://www.greenhouse.cornell.edu/crops/factsheets/fertilizer_cost.pdf. Accessed November 3, 2020.

McCree, K.J. 1971. The action spectrum, absorptance and quantum yield of photosynthesis in crop plants. Agr. Meteor. 9:191–216.

Meyer, G.E., W.W. Troyer, J.B. Fitzgerald, and E.T. Paparozzi E. T., 1992. Leaf nitrogen analysis of poinsettia (*Euphorbia pulcherrima Willd*.) using spectral properties in natural and controlled lighting. Appl. Eng. in Agr. 8(5):715–722.

Moorby, J. and R.T. Besford. 1983. Mineral nutrition and growth. Encycl. of Plant Physiol. New Series 15:481–515.

Munden, R., P.J. Curran, and J.A. Catt. 1994. The relationship between red edge and chlorophyll concentration in the Broadbalk winter wheat experiment at Rothamsted. Remote Sensing 15(3):705–709.

Muñoz-Huerta, R.F., R.G. Guevara-Gonzalez, L.M. Contreras-Medina, I. Torres-Pacheco, J. Prado-Olivarez, and R.V. Ocampo-Velazquez. 2013. A review of methods for sensing the nitrogen status in plants: advantages, disadvantages, and recent advances. Sensors 13(8):10823–10843.

Nemali, K.S. and M.W. van Iersel. 2004. Light intensity and fertilizer concentration: II. Optimal fertilizer solution concentration for species differing in light requirement and growth rate. HortScience 39(6):1293–1297.

Netto, A., E. Campostrini, J.G. De Oliveira, and O.K. Yamanishi. 2002. Portable chlorophyll meter for the quantification of photosynthetic pigments, nitrogen, and the possible use for assessment of the photochemical process in *Carica papaya*. Brazilian J. Plant Physiol. 14:203–210.

Noh, H., Q. Zhang, B. Shin, S. Han, and L. Feng. 2006. A neural network model of maize crop nitrogen stress assessment for a multi-spectral imaging sensor. Biosystems Eng. 94(4): 477–485.

Peñuelas, J., and Filella, I. 1998. Visible and near-infrared reflectance techniques for diagnosing plant physiological status. Trends in Plant Sci. 3(4):151–156.

Pitchay, D.S., J.M. Frantz, J.C. Locke, C.R. Krause, and G.C. Fernandez. 2007. Impact of applied nitrogen concentration on growth of elatior Begonia and New Guinea impatiens and susceptibility of Begonia to *Botrytis cinerea*. J. Amer. Soc. for Hort. Sci. 132(2):193–201.

Pontes, F.V., M.C. Carneiro, D.S. Vaitsman, D. S., G.P. da Rocha, L.I. da Silva, A.A. Neto, and M.I.C. Monteiro. 2009. A simplified version of the total kjeldahl nitrogen method using an ammonia extraction ultrasound-assisted purge-and-trap system and ion chromatography for analyses of geological samples. Analytica Chimica Acta 632(2), 284–288.

Raun, W.R. and G.V. Johnson. 1999. Improving nitrogen use efficiency for cereal production. Agr. J. 91(3):357–363.

Rose, M.A. and J.W. White. 1994. Nitrogen rate and timing of nitrogen application in poinsettia (*Euphorbia pulcherrima* Willd. Ex Klotz.). HortScience 29(11):1309–1313.

Sims, D.A. and J.A. Gamon. 2003. Estimation of vegetation water content and photosynthetic tissue area from spectral reflectance: a comparison of indices based on liquid water and chlorophyll absorption features. Remote Sensing of Environ. 84(4):526–537.

Slater, P.N. and R.D. Jackson. 1982. Atmospheric effects on radiation reflected from soil and vegetation as measured by orbital sensors using various scanning directions. Appl. Optics 21(21):3923–3931.

Sui, R., J.B. Wilkerson, W.E. Hart, L.R. Wilhelm, and D.D. Howard. 2005. Multi-spectral sensor for detection of nitrogen status in cotton. Appl. Eng. in Agr. 21:167–172.

Tewari, V. K., A.K. Arudra, S.P. Kumar, V. Pandey, and N.S. Chandel. 2013. Estimation of plant nitrogen content using digital image processing. Agricultural Eng. Intl: CIGR J.15(2):78-86.

Thomas, J. R. and H.W. Gausman. 1977. Leaf reflectance vs. leaf chlorophyll and carotenoid concentrations for eight crops. Agr. J. 69(5):799–802.

Thomas, J. R. and G.F. Oerther. 1972. Estimating nitrogen content of sweet pepper leaves by reflectance measurements. Agr. J. 64(1):11–13.

Turner, F.T. and M.F. Jund. 1994. Assessing the nitrogen requirements of rice crops with a chlorophyll meter method. Austral. J. Experimental Agr. 34:1001–1005.

Uchida, R. 2005. Essential nutrients for plant growth: nutrient functions and deficiency symptoms. Plant Nutrient Management in Hawaii's Soils. 31-55.

USDA National Agriculture Statistics Service (USDA NASS). 2019. Floriculture Crops 2018 Summary. https://www.nass.usda.gov/Publications/Todays_Reports/reports/floran19.pdf. Accessed November 2, 2020.

Uva, W.F., T.C. Weiler, and R.A. Milligan. 1998. A survey on the planning and adoption of zero runoff subirrigation systems in greenhouse operations. HortScience 33(2):193–196.

van Iersel, M.W., R.B. Beverly, P.A. Thomas, J.G. Latimer. and H.A. Mills. 1998. Fertilizer effects on the growth of impatiens, petunia, salvia, and vinca plug seedlings. HortScience 33(4):678–682.

Woodson, W.R. and J.W. Boodley. 1983. Petiole nitrate concentration as an indicator of geranium nitrogen status. Commun. in Soil Sci. and Plant Anal. 14(5):363–371.

Wright, R.D, K.L. Grueber, and C. Leda. 1990. Medium nutrient extraction with the pour-through and saturated medium extract procedures for poinsettia. HortScience 25(6):658–660.

Xue, L., W. Cao, W. Luo, T. Dai, and Y. Zhu. 2004. Monitoring leaf nitrogen status in rice with canopy spectral reflectance. Agr. J. 96(1):135–142.

Zhu, Y., X. Yao, Y. Tian, X. Liu, and W. Cao. 2008. Analysis of common canopy vegetation indices for indicating leaf nitrogen accumulations in wheat and rice. Intl. J. Appl. Earth Observation and Geoinformation 10(1):1–10.